

Hydrogen Production

Highly Efficient Platinum Group Metal Free Based Membrane-Electrode Assembly for Anion Exchange Membrane Water Electrolysis**

Claudiu C. Pavel, Franco Cecconi, Chiara Emiliani, Serena Santiccioli, Adriana Scaffidi, Stefano Catanorchi, and Massimiliano Comotti*

Abstract: Low-temperature electricity-driven water splitting is an established technology for hydrogen production. However, the two main types, namely proton exchange membrane (PEM) and liquid alkaline electrolysis, have limitations. For instance, PEM electrolysis requires a high amount of costly platinum-group-metal (PGM) catalysts, and liquid alkaline electrolysis is not well suited for intermittent operation. Herein we report a highly efficient alkaline polymer electrolysis design, which uses a membrane-electrode assembly (MEA) based on low-cost transition-metal catalysts and an anion exchange membrane (AEM). This system exhibited similar performance to the one achievable with PGM catalysts. Moreover, it is very suitable for intermittent power operation, durable, and able to efficiently operate at differential pressure up to 3 MPa. This system combines the benefits of PEM and liquid alkaline technologies allowing the scalable production of low-cost hydrogen from renewable sources.

The need to expand the supply of domestically produced energy is a strategic issue because one of the main energy sources, that is, fossil fuels, is often largely imported. In such a domestic production scenario, hydrogen is considered as an excellent energy carrier for renewable and sustainable-based energy systems mainly because of its good energy density and the reversible conversion between hydrogen and electricity.^[1] Moreover, it can be produced by different processes and almost entirely from a large portfolio of diverse domestic and renewable energy sources.^[2–6] Low-temperature water electrolysis has a high potential to cope with the needs of distributed hydrogen production, especially when coupled with renewable electricity sources.^[7] However, to be cost competitive, electrolysis capital and operating costs must be further reduced.

Two technologies are currently widespread: alkaline liquid electrolyte and proton exchange membrane (PEM) water electrolysis.^[8–10] Both of them offer some advantages as

well as some limitations. Liquid alkaline electrolysis for instance, is a very robust technique and employs non-precious metal or oxides as electro-catalysts. However, it is not very suitable for intermittent power operation since its balance of plant is quite complex and difficult to manage under these circumstances. On the other hand, PEM electrolysis would represent a good solution for intermittent power operation, and offers higher energy density. However, the acidic environment limits the catalysts to noble metals, resulting in high cost.

Low capital and operating costs could be achieved by combining opportunely the benefits of the two technologies. Attempts of this kind have been mainly reported for alkaline membrane fuel cell,^[11–14] and only very recently and to a limited extent for water electrolysis.^[15] In water electrolysis, a system based on PGM catalysts combined with an anion exchange membrane (AEM) has been described which showed high efficiency but a very poor stability, mainly due to ionomer and membrane electrode-assembly (MEA) instability.^[15] Herein we report a highly efficient and durable alkaline polymer electrolysis design, which uses a MEA based on low-cost transition-metal catalysts and an AEM.

The employed cell architecture is shown in Figure 1. The anodic and cathodic half cells are separated by an anion exchange membrane, in the presence of middle alkaline electrolyte solution circulating only through the anodic half-cell. The alkaline environment has been obtained by using

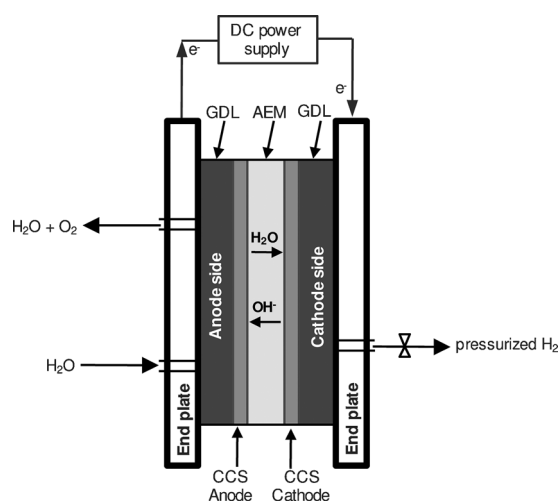


Figure 1. Schematic representation of the AEM water electrolysis cell. GDL = gas diffusion layer.

[*] Dr. C. C. Pavel, F. Cecconi, Dr. C. Emiliani, S. Santiccioli, Dr. A. Scaffidi, S. Catanorchi, Dr. M. Comotti
R&D Department, Acta SpA
Via di Lavoria 56G, 56040, Crespina (PI) (Italy)
E-mail: m.comotti@actaspa.com
Homepage: <http://www.actaspa.com>

[**] We thank the Tokuyama Corporation for providing the A-201 membrane and for the fruitful collaboration.

Supporting information for this article is available on the WWW under <http://dx.doi.org/10.1002/anie.201308099>.

a basic solution in combination with the anion exchange membrane (A-201 from Tokuyama Corporation). However, unlike conventional liquid alkaline technology,^[8] the concentrated KOH solution was replaced by diluted carbonate/bicarbonate aqueous solution, such as 1 wt. % K_2CO_3 or 1 wt. % $\text{K}_2\text{CO}_3/\text{KHCO}_3$ (0.67% and 0.33%, respectively). This setup offers several benefits which are going to influence both electrolyzer efficiency and capital cost. In fact, the electrolyte loop does not need to be sealed to avoid carbonation (i.e. the electrolyte is unaffected by CO_2 contamination). Moreover, the middle alkaline electrolyte (pH 10–11) is a less-aggressive medium in comparison with concentrated KOH solution, strongly decreasing the degradation occurring to the anion exchange membranes.^[16,17]

The hydrogen- and oxygen-evolution catalysts employed within this study are commercially available materials named ACTA 4030 and 3030, respectively, manufactured by Acta SpA. These materials are based on $\text{Ni}/(\text{CeO}_2\text{-La}_2\text{O}_3)/\text{C}$ and CuCoO_x mixed oxides, respectively, and have been designed to properly perform in a middle alkaline environment. A detailed description and characterization of the catalysts can be found in the Experimental Section and the Supporting Information. Cathode and anode electrodes were prepared by the catalyst-coated substrate (CCS) method, and the MEA was obtained in situ by filter pressing all the cell components as described in the Supporting Information.

It is established that the kinetics of oxygen-evolution reaction (OER) as well as oxygen-reduction reaction (ORR) are sluggish even in alkaline media.^[18–20] As a consequence and because of the electrode-manufacturing method employed, an anode catalyst loading of 36 mg cm^{-2} has been used, and kept as a fix parameter within this work. On the other side, it was observed that the catalyst loading on the cathode electrode had a great influence on the cell performance. Catalyst loading was varied from 0.6 to 7.4 mg cm^{-2} , resulting in cell potential ranging between 2.01 and 1.89 V at 470 mA cm^{-2} and 316 K, respectively, (Figure 2a).

Notably, for the highest catalyst loading used, a system efficiency as high as $4.02\text{ kWh Nm}^{-3}\text{ H}_2$ could be achieved. The measured alternating-current (AC) resistance at 1 kHz ^[21] varied between 0.218 and $0.132\text{ }\Omega\text{ cm}^2$ at 470 mA cm^{-2} and 316 K for catalyst loading ranging between 0.6 to 7.4 mg cm^{-2} , respectively. Although this parameter should mainly reflect the contribution of the membrane and the diffusion media,^[22] in all experiments the only variable was the hydrogen-evolution reaction (HER) catalyst loading. Consequently, the measured differences could be addressed to the effect of different HER catalyst loading.

To better analyze the catalysts and thus the kinetic contribution to the cell potential, studies were carried out on two systems characterized by different HER catalyst loading (i.e. 0.6 mg cm^{-2} and 4.8 mg cm^{-2}). *iR*-free voltages were gathered by measuring online the AC resistance (Figure 2b), as reported in the Supporting Information. These data further confirmed the influence of HER catalyst loading on the ohmic contribution. In fact, the measured resistance varied from 0.506 to $0.206\text{ }\Omega\text{ cm}^2$ (at 5 and 625 mA cm^{-2} , respectively) and from 0.480 to $0.172\text{ }\Omega\text{ cm}^2$ (at 5 and 625 mA cm^{-2} , respectively) for the system having 0.6 and

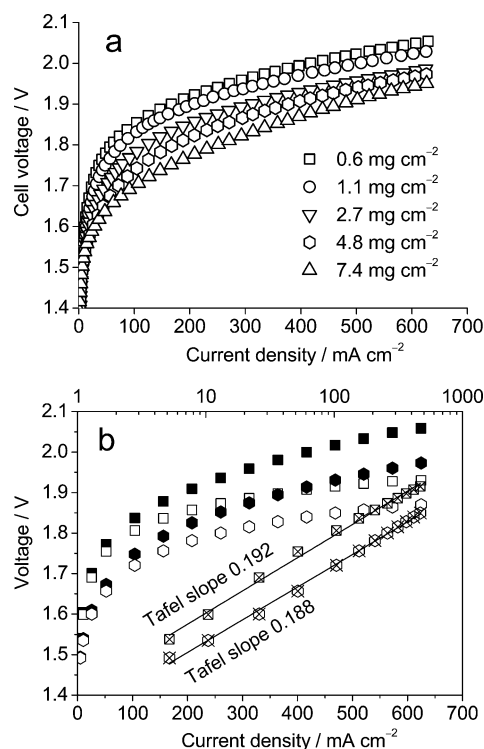


Figure 2. a) Polarization curves recorded after 24 h test run for AEM water electrolysis cell containing MEAs with different HER catalyst loading. b) Original un-corrected (solid symbol) and ohmically (i.e., *iR*-free) corrected (open symbols) polarization curves for two different HER catalyst loadings: 0.6 mg cm^{-2} (square symbols) and 4.8 mg cm^{-2} (hexagon symbols). Tafel slopes are described as linear fitting of *iR*-free voltage data (crossed symbols) plotted on logarithmic scale (top x axes). Tests were performed using K_2CO_3 (1 wt. %) electrolyte at 316 K and 0.1 MPa.

4.8 mg cm^{-2} HER catalyst loading, respectively. The obtained *iR*-free potential was then fitted by means of Tafel equation in the $5.2\text{--}470\text{ mA cm}^{-2}$ current density range. Tafel slopes close to $190\text{ mV decade}^{-1}$ were derived from both HER loadings at 316 K and 0.1 MPa (Figure 2b). A comparison of these data with data reported in the literature is not straightforward. In fact, whereas reaction mechanisms and Tafel slopes are to a certain extent established for the OER and HER in acidic conditions with PGM based catalysts,^[23] these are not for first-row transition-metal oxide catalysts in alkaline conditions. On this matter, despite some efforts, the reaction mechanism remains controversial, making data analysis and comparison very difficult, especially when these are achieved under different experimental conditions.^[24]

The system behavior was studied under transitory operation regimes as well. With this aim, cells with different HER catalyst loadings were subjected to cycles. In a typical test (Figure S1a in the Supporting Information) six alternating start/stops cycles were applied to the cell. Current was instantly ramped from zero to the operating value (i.e. 470 mA cm^{-2}) without limiting the cell potential, and then left to the operating current for 40 min. Afterward, the current flow was stopped and the cell was left in floating mode. The cycles profile was found to be very reproducible both in terms

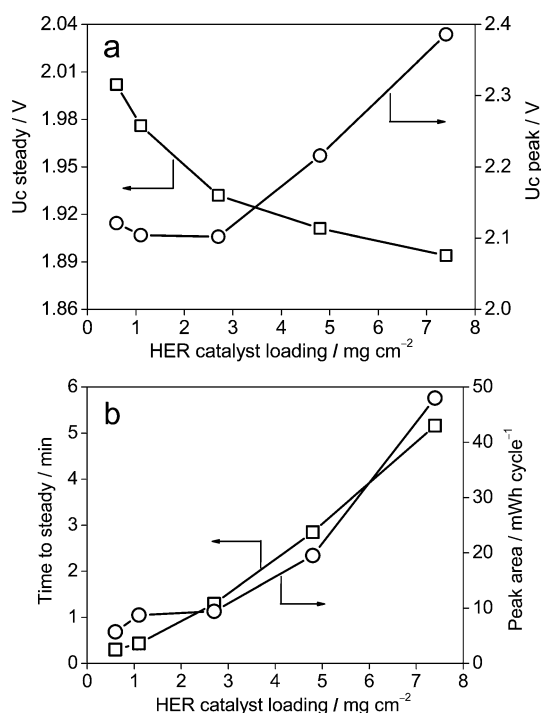


Figure 3. AEM cell performance under cycling testing conditions. Results are expressed as a) cell potential in steady conditions ($U_{c, \text{steady}}$), peak potential during cell start-up ($U_{c, \text{peak}}$) and b) time to steady potential and peak area versus HER catalyst loading. Tests were performed with K_2CO_3 (1 wt. %) electrolyte at 316 K.

of peak potential and peak area (Figure S1b). Additionally, a comprehensive summary of these studies is reported in Figure 3.

The HER catalyst loading strongly influences the cell potential during steady state operation. Additionally, peak potential was found to be strongly dependent on this parameter as well (Figure 3a). In particular, peak potential varied from approximately 2.1 to approximately 2.4 V for HER catalyst loadings between 0.6 and 7.4 mg cm^{-2} , respectively. A very strong influence was also found on peak area and time to steady (the time to steady indicates the time required to reach cell potential typical of steady state operation). In particular, both peak area and time to steady varied almost linearly with catalyst loading. Remarkably, in all cases the system reached steady-state conditions in less than 10 min. These findings might be correlated with catalyst loading and thus cathode thickness. Noticeably, in the worst case which corresponds to the highest HER catalyst loading (7.4 mg cm^{-2}), peak area and thus energy loss was below 45 mWh cycle^{-1} , representing about 0.6% of the system energy requirement in steady-state conditions. In a realistic scenario, maximum cell potential could be limited to a lower value (e.g. 2.10–2.20 V) when starting the system. Under these specifications, the target hydrogen production flow (i.e. obtained at the current density of 470 mA cm^{-2}) would be achieved in less than one minute, without any additional energy consumption. Consequently, this aspect makes this technology extremely suitable for intermittent operations as required by renewable energy sources.

The effect of different electrolytes on cell performance was also studied for the system with a cathode loading equal to 7.4 mg cm^{-2} (Figure S2). Differences were somehow reduced for a system operating with 1 wt. % K_2CO_3 or 1 wt. % $\text{K}_2\text{CO}_3/\text{KHCO}_3$ aqueous solution, characterized by similar conductivities and pH values (15.8 mS cm^{-1} and pH 11.2 versus 12.9 mS cm^{-1} and pH 10.2, respectively). In contrast, the cell potential dropped when a 1M KOH solution (194 mS cm^{-1} and pH 14) was used as electrolyte. In this case, cell potential as low as 1.79 V was recorded at 316 K and 470 mA cm^{-2} . Measured AC resistance varied consequently with values corresponding to 0.151, 0.132, and 0.087 $\Omega \text{ cm}^2$ for system working with 1 wt. % $\text{K}_2\text{CO}_3/\text{KHCO}_3$, 1 wt. % K_2CO_3 , and 1M KOH electrolytes, respectively. However, the ohmic penalty due to the lower conductivity of the bicarbonate versus the hydroxide ions did not result in a very large potential difference (i.e. 130 mV at 470 mA cm^{-2}). Finally, though a lower cell potential was recorded when using a 1M KOH solution, stability issues might rise over time because of membrane degradation, as reported for other systems.^[16,17] Consequently, further investigations with this electrolyte were not carried out.

The effect of temperature on cell potential was also studied (Figure S3). As expected, the temperature has a great effect on system efficiency. In particular, cell potential as low as 1.81 V at current density of 470 mA cm^{-2} and 328 K was recorded. This corresponds to an efficiency of 3.85 $\text{kWh Nm}^{-3} \text{ H}_2$. Moreover, a linear correlation between cell potential and temperature was found (Figure S3b). Remarkably, this system showed comparable performance to the one obtained by Leng and co-workers.^[15] In fact, the cell potential of 1.82 V (at 400 mA cm^{-2}) extrapolated at 323 K, is comparable with the best data obtained by Leng and co-workers (1.80 V at 400 mA cm^{-2} and 323 K).^[15] However, it has to be mentioned that in the study of Leng and co-workers the best performance was a spot data (measured within the first hour of operation) since the system was affected by a very poor stability (i.e. after a few hours of operation the cell potential raised to 2.2 V or higher values). Additionally, the MEA was fabricated with rather high loadings of PGM electro-catalysts, whereas cost-effective alternatives were used in our work. Thus, this represents a huge improvement since similar operating costs could be achieved with much lower capital investments.

System stability was studied as well (Figure 4). Durability tests were performed at a constant differential pressure of 3 MPa for systems with HER catalyst loading equal to 7.4 mg cm^{-2} using two different $\text{K}_2\text{CO}_3/\text{KHCO}_3$ and K_2CO_3 aqueous solutions. A good stability was generally observed. In both cases, cell potential reached 2.05 V after 1000 h of continuous operation. Furthermore, the cell potential did not change appreciably for both systems from 800 h to the end of the test. This represents a big improvement in comparison with the durability of the system described by Leng and co-workers.^[15] The plots reported in Figure 4 are the same with the exception of the first 300 working hours. These slight differences could be related to the electrolyte employed. In fact, the 1 wt. % K_2CO_3 solution has initially a slightly higher pH value and conductivity in comparison with the 1 wt. %

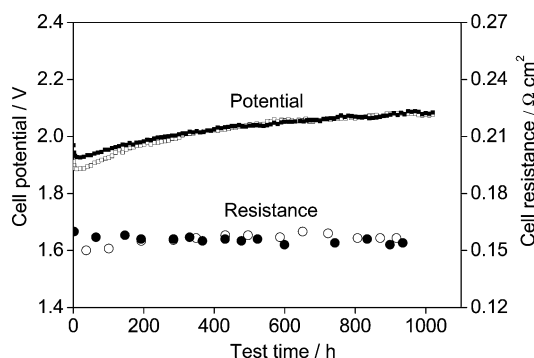


Figure 4. Long-term performance and AC resistance (1 kHz) of AEM water electrolysis cells pressured at 3 MPa operating with 1 wt. % $\text{K}_2\text{CO}_3/\text{KHCO}_3$ (solid symbol) and 1 wt. % K_2CO_3 (open symbols) electrolyte solutions. Tests were performed on cells having a HER catalyst loading of 7.4 mg cm^{-2} , at constant current density of 470 mA cm^{-2} and 316 K.

$\text{K}_2\text{CO}_3/\text{KHCO}_3$ solution. However, the 1 wt. % K_2CO_3 solution undergoes to a slight carbonation within the first 300 h, reaching a similar pH value and conductivity to the $\text{K}_2\text{CO}_3/\text{KHCO}_3$ solution. As a consequence, after this time, the cell potential for both systems is almost identical. This fact is further confirmed by the measured AC cell resistance, which reached similar values (as noticed for the cell potential) after 300 h of continuous operation.

In conclusion, our study describes a novel AEM alkaline water electrolysis system which offers several advantages over conventional and established technologies. The system employs an anion exchange membrane and cost-effective transition-metal catalysts, which effectively operates with a CO_2 tolerant and less aggressive alkaline electrolyte. This novel technology was proved to be very efficient, durable, and reliable under continuous and intermittent operation modes, allowing in principle the scalable production of low-cost hydrogen also from renewable sources.

Experimental Section

Acta's 3030 (<http://www.actaspa.com/products/>) commercial material was used as anode catalyst for oxygen evolution reaction (OER). This material consists in a CuCoO_x , synthesized by co-precipitation of $\text{Co}(\text{NO}_3)_2 \cdot 6\text{H}_2\text{O}$ and $\text{CuSO}_4 \cdot 5\text{H}_2\text{O}$. From X-ray diffraction analysis the as-synthesized material was found to be a crystalline pure-phase with spinel structure indexed by space group $Fd3m$ (Figure S4). The BET surface area of CuCoO_x material was ca. $100 \text{ m}^2 \text{ g}^{-1}$ as determined from nitrogen physisorption measurement (using a Quadrasorb SI instrument from Quantachrome) with pore volume of $0.35 \text{ cm}^3 \text{ g}^{-1}$.

Acta's 4030 commercial catalyst was used as cathode for hydrogen evolution reaction (HER). This is a nickel-based nanostructured material with the transition-metal deposited on $\text{CeO}_2\text{-La}_2\text{O}_3$ /carbon support. The synthesis consists in two steps: 1) preparation of the support by deposition of inorganic Ce and La precursors on carbon, followed by calcination, and 2) deposition-precipitation of Ni hydroxide onto the $\text{CeO}_2 + \text{La}_2\text{O}_3$ /carbon support, followed by reduction. The material obtained is highly porous with a BET surface area of $180 \text{ m}^2 \text{ g}^{-1}$ and pore volume of $0.59 \text{ cm}^3 \text{ g}^{-1}$. It contains Ni crystallite

with size of 17 nm as determined from the XRD peak width (Figure S4).

A201 membrane (from Tokuyama Corporation, Japan) was used as anion exchange membrane for all experiments. This membrane has a thickness of $28 \mu\text{m}$ (in dry form) and is characterized by an ion exchange capacity of 1.8 mmol g^{-1} , water uptake of 30%, and ion conductivity of 12 mS cm^{-1} (HCO_3^- form).

The cell potential and currents were controlled and monitored by an automatic multi-channel Arbin testing system (Arbin Instruments, USA) operated by MITS Pro software.

Additional information on electrode and MEA fabrication, as well as testing details can be found in the Supporting Information.

Received: September 15, 2013

Published online: December 13, 2013

Keywords: anion exchange membrane · hydrogen · electrocatalysis · water splitting

- [1] J. A. Turner, *Science* **2004**, 305, 972.
- [2] I. Dincer, C. Zamfirescu, *Int. J. Hydrogen Energy* **2012**, 37, 16266.
- [3] A. Milbrandt, M. Mann, Tech. Rep. TP-560-42773, **2009**, NREL.
- [4] J. A. Funk, *Int. J. Hydrogen Energy* **2001**, 26, 185.
- [5] P. C. Hallenbeck, J. R. Benemann, *Int. J. Hydrogen Energy* **2002**, 27, 1185.
- [6] M. Ni, M. K. H. Leung, D. Y. C. Leung, K. Sumathy, *Renewable Sustainable Energy Rev.* **2007**, 11, 401.
- [7] M. Balat, *Int. J. Hydrogen Energy* **2008**, 33, 4013.
- [8] T. Smolinka in *Encyclopedia of electrochemical power sources*, Vol. 3 (Eds.: J. Garche, C. K. Dyer, P. T. Moseley, Z. Ogumi, D. A. J. Rand, B. Scrosati), Elsevier B.V., Amsterdam, **2009**, pp. 394–413.
- [9] K. Zeng, D. Zhang, *Prog. Energy Combust. Sci.* **2010**, 36, 307.
- [10] F. Barbir, *Sol. Energy* **2005**, 78, 661.
- [11] A. Filpi, M. Boccia, H. A. Gasteiger, *ECS Trans.* **2008**, 16, 1835.
- [12] M. Piana, S. Catanorchi, H. A. Gasteiger, *ECS Trans.* **2008**, 16, 2045.
- [13] M. Piana, M. Boccia, A. Filpi, E. Flammia, H. A. Miller, M. Orsini, F. Salusti, S. Santiccioli, F. Ciardelli, A. Pucci, *J. Power Sources* **2010**, 195, 5875.
- [14] M. Faraj, E. Elia, M. Boccia, A. Filpi, A. Pucci, F. Ciardelli, *J. Polym. Sci. Part A* **2011**, 49, 3437.
- [15] Y. Leng, G. Chen, A. J. Mendoza, T. B. Tighe, M. A. Hickner, C.-Y. Wang, *J. Am. Chem. Soc.* **2012**, 134, 9054.
- [16] S. Maurya, S.-H. Shin, M.-K. Kim, S.-H. Yun, S.-H. Moon, *J. Membr. Sci.* **2013**, 443, 28.
- [17] G. Merle, M. Wessling, K. Nijmijer, *J. Membr. Sci.* **2011**, 377, 1.
- [18] J. Rossmeisl, Z.-W. Qu, H. Zhu, G.-J. Kroes, J. K. Nørskov, *J. Electroanal. Chem.* **2007**, 607, 83.
- [19] J. Suntivich, K. J. May, H. A. Gasteiger, J. B. Goodenough, Y. Shao-Horn, *Science* **2011**, 334, 1383.
- [20] H. A. Gasteiger, N. M. Markovic, *Science* **2009**, 324, 48.
- [21] K. R. Cooper, M. Smith, *J. Power Sources* **2006**, 160, 1088.
- [22] H. A. Gasteiger, S. S. Kocha, B. Sompalli, F. T. Wagner, *Appl. Catal. B* **2005**, 56, 9.
- [23] J. C. Cruz, V. Baglio, S. Siracusano, V. Antonucci, A. S. Aricò, R. Ornelas, L. Ortiz-Frade, G. Osorio-Monreal, S. M. Durón-Torres, L. G. Arriaga, *Int. J. Electrochem. Sci.* **2011**, 6, 6607.
- [24] M. E. G. Lyons, R. L. Doyle, *Int. J. Electrochem. Sci.* **2012**, 7, 9488.